Werk

Jahr: 1980
Kollektion: fid.geo
Signatur: 8 Z NAT 2148:48
Digitalisiert: Niedersächsische Staats- und Universitätsbibliothek Göttingen
Werk Id: PPN1015067948_0048
PURL: http://resolver.sub.uni-goettingen.de/purl?PPN1015067948_0048

LOG Id: LOG_0026
LOG Titel: Load-induced stresses and their relation to the initial stress field
LOG Typ: article

Übergeordnetes Werk

Werk Id: PPN1015067948
PURL: http://resolver.sub.uni-goettingen.de/purl?PPN1015067948
OPAC: http://opac.sub.uni-goettingen.de/DB=1/PPN?PPN=1015067948

Contact

Niedersächsische Staats- und Universitätsbibliothek Göttingen
Georg-August-Universität Göttingen
Platz der Göttinger Sieben 1
37073 Göttingen
Germany
Email: gdz@sub.uni-goettingen.de

J. Geophys. 48, 94–100, 1980

Journal of Geophysics

Load-Induced Stresses and Their Relation to the Initial Stress Field

G. Bock*
Geophysikalisches Institut, Universität Karlsruhe, Hertzstr. 16, D-7500 Karlsruhe 21, Federal Republic of Germany

Abstract. The additional stresses under a reservoir are computed by the analytical integration of the Boussinesq equations. Expressions are given for (1) a constant and (2) a linearly varying vertical load over a rectangular area. Given the direction of the primary stress field a simple calculation can be performed to check whether the additional stresses drive the total stress field towards the limiting failure threshold or not. This is demonstrated by a model lake of three-dimensional geometry. It is shown that not only in the case of normal faulting, but also in the case of thrust and transcurrent mechanisms, stresses are changed in the direction favourable for the occurrence of earthquakes by the water load alone. An application of the method to the seismic observations at the Schlegeis-Reservoir, Austria, indicates that a thrust-type mechanism of the seismic events as postulated in an earlier model is not compatible with the results of the theoretical calculations.

Key words: Initial stress field – Reservoir induced seismicity – Failure mechanism.

Introduction

Up to now more than 30 cases are known where changes of the natural seismicity are probably caused by the filling of large reservoirs (Simpson 1976; Gupta and Rastogi 1976). Earthquakes associated with dams cover a wide magnitude range, with an upper limit, as far observed, of about 6.25. Destructive ones like in Koyna, India, (Gupta et al. 1969) and Kremasta, Greece, (Comninakis et al. 1968) as well as minor earthquakes and changes in micro-earthquake activity have been related to the presence of artificial lakes. For a review see Simpson (1976). As indicated by observations at several sites, filling of a reservoir may even bring about a decrease of the natural seismicity (Simpson 1976; Bufe 1976). In spite of this diversity of the characteristic features of reservoir induced seismicity only two mechanisms are mainly discussed (Kisslinger 1976): Earthquakes near reservoirs can be triggered (1) by the incremental stresses induced by the water load (e.g., Gough and Gough 1970b) and (2) as a result of reservoir water migrating into the rock and increasing the pore pressure, which reduces the effective stresses (Hubert and Rubey 1959) thus facilitating failure. The last mechanism has also been proposed to explain the occurrence of seismic events associated with fluid injections into deep wells (e.g. Raleigh et al. 1976). According to Kisslinger (1976) a consensus is emerging that the increasing pore pressure is the most important factor controlling induced seismicity associated with dams. But no mechanism can be rejected up to now. In all cases the initial stress field must be already close enough to the limiting failure stress so that additional forces due to the reservoir, which are relatively low compared with the primary ones, are sufficient to trigger an earthquake. This idea is confirmed by fault-plane solutions of induced earthquakes which are consistent with the regional stress field.

In this paper the modification of the primary stress field by the water load is discussed. Several authors have described methods for the computation of the incremental stresses under artificial lakes (Gough 1969; Gough and Gough 1970a; Lee 1972; Nyland and Withers 1976; Withers and Nyland 1976). The modification of the initial tectonic stress field by the water load has been discussed by Snow (1972). Following Snow, earthquakes may be triggered by the load only in tectonic environments of normal faulting whereas transcurrent and thrust faults are stabilized. In his discussion Snow assumes a lake extended infinitely in the horizontal directions. Taking into account a lake with finite dimensions it may be imagined, however, that also earthquakes with strike slip and overthrust mechanism can be triggered by the water load. Recently, this has been demonstrated by Bell and Nur (1978) with two-dimensional lake models. It is the goal of this paper to illustrate the modification of the primary stress field by water loads with three-dimensional geometry.

Method of Computation

One method for the computation of the incremental elastic stresses under a lake of arbitrary shape has been presented by Gough and Gough (1970a). The water load of the lake is approximated by an array of vertical point forces which act at the surface of an elastic, homogeneous and isotropic halfspace. At a point within the halfspace the stresses due to one point force are given by the Boussinesq-equations. The total stress field is obtained by summation over all point forces. In this computation scheme singularities arise at the origin of the point forces. Therefore, the calculation of stresses is inaccurate at points situated close to the bottom of the lake. One method to

Contribution No. 221 of the Geophysical Institute, University of Karlsruhe. Sonderforschungsbereich Felsmechanik of Karlsruhe University

* *Present address:* Research School of Earth Sciences, Australian National University, P.O. Box 4, Canberra ACT 2600, Australia

0340-062X/80/0048/0094/$01.40

avoid these singularities makes use of spatially harmonic surface loads and the Fourier transform of the lake depth (Nyland and Withers 1976). Another method is the analytical integration of the Boussinesq-equations over areas of known load distributions. This concept has been applied in the present study. It proved to be very efficient in the computation of simple geometrical lake models as presented in a later section. The results of the analytical integration are given in the appendix for the following two load distributions over a rectangular area: (a) constant load and (b) linearly varying load. In the cartesian coordinate system used, x points to the East, y to the North and z in downward direction (left-handed system). To allow for other directions a local coordinate system x', y', z' is also introduced. In this x' is tangent to the lake bottom in the direction of increasing load, if case (b) of the above mentioned load distributions is investigated. The z' direction may be different from the z direction by an angle ψ which describes the dip of the lake bottom. The y'-axis is horizontal. If φ denotes the angle between the y- and y'-direction a point with coordinates (x, y, z) in the first system will have coordinates $(x' y', z')$ in the local system, given by

$$\begin{pmatrix} x' \\ y' \\ z' \end{pmatrix} = A \begin{pmatrix} x \\ y \\ z \end{pmatrix}.$$

The 3×3 transformation matrix A is given by

$$A = \begin{pmatrix} -\sin\varphi\cos\psi & \cos\varphi\cos\psi & -\sin\psi \\ \cos\varphi & \sin\varphi & 0 \\ -\sin\varphi\sin\psi & \cos\varphi\sin\psi & \cos\psi \end{pmatrix}.$$

The components of the stress tensor are computed in the local (x', y', z')-system. The stress tensor S in the (x, y, z)-system is obtained from the stress tensor S' in the local system by the transformation equation

$$S = A^T S' A$$

where T means transposition. The total stress field is obtained by summation over all elements by which the water load of the lake is approximated.

It is desirable now to compare this stress field with the initial one. In most cases nothing is known about the primary stress field. From geological and seismological observations, however, sometimes its direction can be deduced. Then a simple numerical calculation can be carried out to check whether the filling of a reservoir drives the stresses towards the failure envelope in a Mohr diagram or not. If σ_{10} and σ_{30} denote the greatest and least compressional stress and a_1, b_1, c_1 and a_3, b_3, c_3 their direction cosines in the (x, y, z)-system, the additional stresses in σ_{10} and σ_{30} direction are given by:

$\Delta\sigma_i = a_i^2\sigma_x + b_i^2\sigma_y + c_i^2\sigma_z + 2b_i c_i \tau_{yz} + 2c_i a_i \tau_{xz} + 2a_i b_i \tau_{xy}$ $(i=1$ and $3)$

σ_x, σ_y, σ_z, τ_{xy}, τ_{xz}, τ_{xy} are the stress components at a field point in the halfspace due to the water load. The Mohr circle of stress moves away from the failure envelope (stabilization) if

$$\frac{\Delta\sigma_3}{\Delta\sigma_1} > \frac{1-\sin\phi}{1+\sin\phi} \qquad \text{(A)}$$

and moves towards the failure envelope (destabilization) if

$$\frac{\Delta\sigma_3}{\Delta\sigma_1} < \frac{1-\sin\phi}{1+\sin\phi} \qquad \text{(B)}$$

(Snow 1972). For deriving these relations the Mohr envelope of failure is approximated by a straight line. Its slope is given by the angle of internal friction ϕ, which for rocks is commonly less than 45° (e.g. Handin 1966). Condition B is equivalent to the condition that $\Delta\tau/\Delta\sigma$ rises above $\tan\phi$. $\Delta\tau/\Delta\sigma$ is the ratio of the shear to the normal stress across a plane passing through the direction of the intermediate principal stress and making an angle $\pi/4-\phi/2$ with the direction of σ_{10}. Knowing the orientation of the fault plane and the slip vector in an earthquake, this ratio can be calculated without assuming the direction of the initial stress field. In the examples of the next section the change $\Delta\tau_0$ of the initial maximum shear stress $\tau_0 = 0.5(\sigma_{10}-\sigma_{30})$ has been chosen as parameter describing the measure of stabilization or destabilization:

$$\Delta\tau_0 = 0.5(\Delta\sigma_1 - \Delta\sigma_3)$$

$\Delta\tau_0$ is a meaningful quantity, if it is small compared with τ_0, i.e., if the additional stress field is much weaker than the initial stress field. $\Delta\tau_0$ is between $-\tau_{max}$ and $+\tau_{max}$ where τ_{max} denotes the maximum shear stress induced by the water load. The initial maximum shear stress τ_0 is always increased, if condition B is fulfilled (compression reckoned positive). Condition A can be connected with both positive and negative values of $\Delta\tau_0$ (if $\phi > 0$).

A Simple Geometrical Model

A simple three-dimensional model has been studied to test the method. This model is a lake of rectangular cross section (Figs. 1-3). The length of the lake is 0.8 km, the width is 0.2 km and the maximum water depth is 100 m. The stresses are symmetrical about the two vertical planes which cross the lake at the horizontal centre lines. A value of 30° has been chosen for the angle of internal friction of the crustal rock. The distribution of the additional stress $\Delta\tau_0$ in the direction of the initial maximum shear stress τ_0 is shown in Figs. 1–3 for different initial stress directions. They represent tectonic environments of normal, thrust and transcurrent faulting. The regions in which the stresses move towards the failure envelope (i.e., condition B is fulfilled) are emphasized by the stippled pattern.

In a region of normal faulting the zones destabilized by the water load are situated below the lake bottom (Fig. 1). It is remarkable to note that the likelihood for failure is less directly below the lake compared with greater depths. At depths greater than about one third of the lake width the risk for failure increases. There the initial maximum shear stress τ_0 is increased by more than 3 bar. In regions situated farther away from the lake τ_0 is decreased by more than 0.5 bar. It is unlikely that there an earthquake of normal faulting mechanism is triggered by the water load alone. Nevertheless, it could be triggered by the increasing pore pressure (Simpson 1976).

For thrust faulting, the likelihood of failure is increased in regions situated very close to the surface and extending landwards (Fig. 2). Epicenters of overthrusting earthquakes induced by the water load alone would be located outside the reservoir region. The focal depths would be very shallow. The extension of the destabilized volume increases with the lake width. Thus focal depths could be of the order of 1 km if the lake width is of the order of several kilometers. The increase of τ_0 is much less

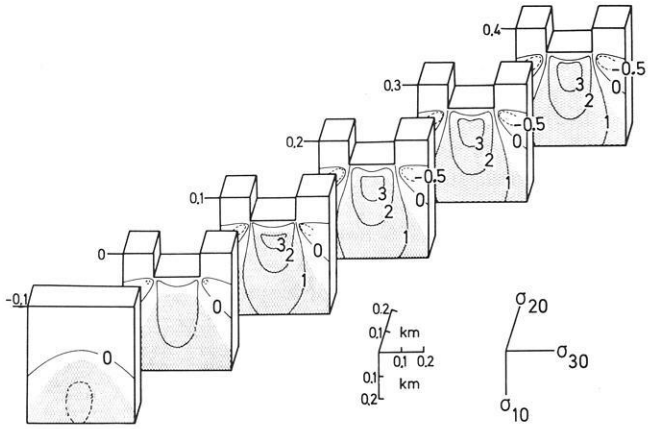

Fig. 1. Change of initial maximum shear stress in bar, in a tectonic environment of normal faulting under a lake of rectangular cross section, 0.2 km wide, 0.8 km long and 100 m deep. Regions destabilized by the water load are *stippled*. Angle of internal friction = 30°

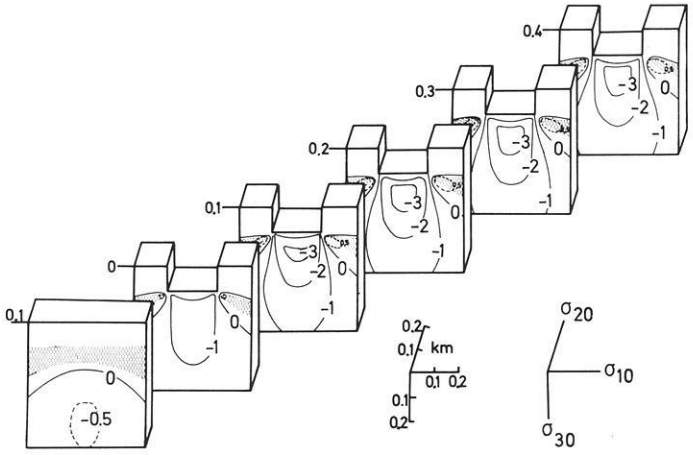

Fig. 2. Same as Fig. 1, for a tectonic environment of thrust faulting

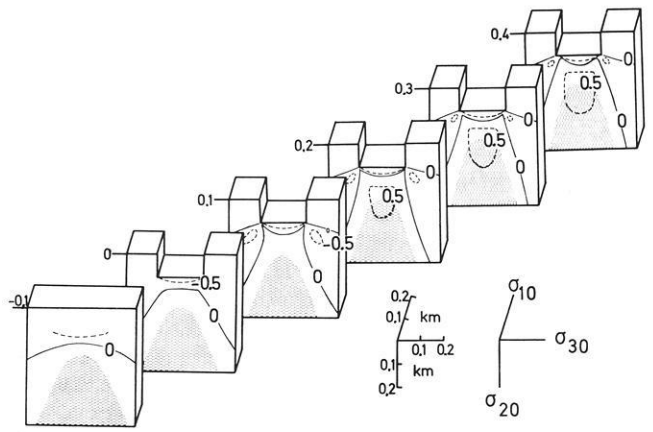

Fig. 3. Same as Fig. 1, for a tectonic environment of transcurrent faulting

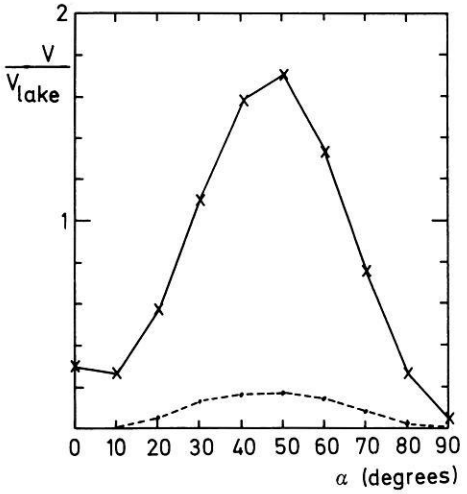

Fig. 4. Volume destabilized in a tectonic environment of transcurrent faulting under a lake of rectangular cross section and 100 m deep. Length and width of the lake are in the ratio 4:1. The volume is normalized to the volume of the lake. *Full line:* volume with $\Delta\tau_0 \geqq 0.5$ bar; *broken line:* volume with $\Delta\tau_0 \geqq 1$ bar. α is the angle between the direction of the greatest principal compressional stress and the longer axis of the lake

than in a normal faulting region; its maximum value is about 0.5 bar. The crustal parts situated below the reservoir region are stabilized in a thrust faulting stress regime.

In a third example an initial stress field has been assumed which favours transcurrent faulting (Fig. 3). In this case the likelihood of failure increases in regions which are situated below the reservoir. However, as in the case of normal faulting the very shallow parts of the crustal rocks are less subjected to failure than the deeper parts. The transition to the destabilized region occurs approximately at a depth of two thirds of the lake width. In the example presented the lake width is 0.2 km and the stresses approach the failure envelope at depths greater than 0.13 km below the bottom of the lake. If the lake width is 3 km this depth is 2 km. For transcurrent faulting, the volume destabilized by the water load depends strongly on the direction of the greatest principal compressional stress σ_{10} with respect to the longer axis of the reservoir. In the example of Fig. 3 both directions are identical. The variation of the destabilized volume with the direction of σ_{10} is shown in Fig. 4. It reaches a maximum value if the angle α between the longer axis of the lake and σ_{10} is between 40 and 60°. Already for $\alpha > 10°$ τ_0 is increased by more than 1 bar (broken line). The example of Fig. 3 corresponds to $\alpha = 0°$ in Fig. 4.

An Example (Schlegeis-Reservoir, Austria)

The Schlegeis arch buttress dam on the Zemm river was completed in 1971. The height of the dam is 131 m. The storage volume of the reservoir is 127.7×10^6 m^3 (Widmann et al. 1972). Continuous seismic monitoring was started in 1971 by a short period vertical station (Blum and Fuchs 1974). Localization of seismic events was made possible by additional stations installed temporarily in the vicinity of the dam (Blum et al. 1977). The local seismic activity observed is characterized by numerous weak tremors ($M_L < 0$) occurring during periods of lowering water level. During periods of rising and maximum water level

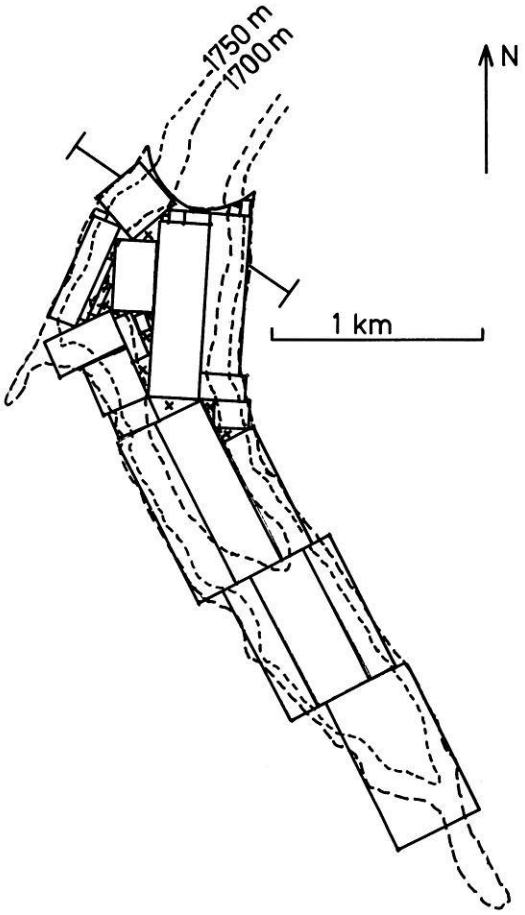

Fig. 5. Schlegeis-Reservoir, approximation of the water load and *contour lines* given in intervals of 50 m. Maximum lake level is reached at 1782 m. *Crosses* mark single point forces

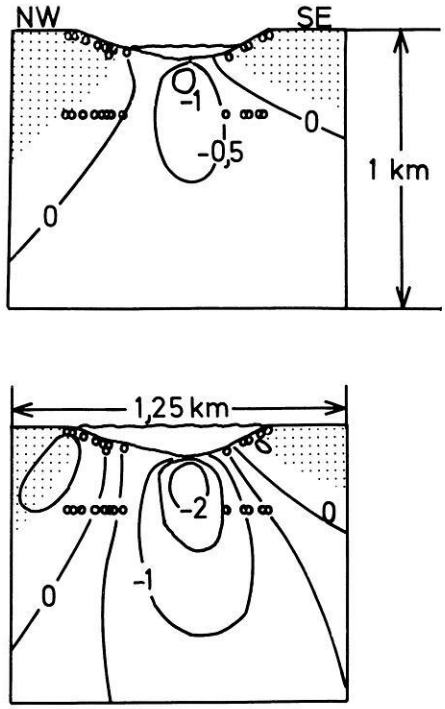

Fig. 6. Change of the initial maximum shear stress along a vertical cross section under the Schlegeis-Reservoir. The position of the section is given in Fig. 5. Stresses are in bar. *Upper part:* water level at 1722 m, *lower part:* at 1782 m. *Stippled:* regions destabilized by the filling of the reservoir. Angle of internal friction = 30°. *Circles* denote the position of hypocenters in the vicinity of the cross section. Both, the maximum (lower row of *circles*) and minimum (upper row of circles close to the surface) possible focal depth of each tremor is shown as calculated by Blum (1975)

local seismic activity is relatively low. A detailed description of the seismic phenomena observed until 1975 has been given by Blum (1975). Since then the periodic occurrence of the local seismic activity did not change. Hypocenters of local tremors could be determined for the period March–April 1974 (Blum 1975; Blum et al. 1977). Focal depths are very shallow (< 300 m) and the epicenters were located clearly outside the region of greatest water depth. Focal mechanism data are not available. Blum et al. (1977) proposed a model of dynamic stress equilibrium to explain the tremor mechanism. They assumed a tectonic environment of thrust faulting with the greatest compressional stress steadily increasing. The upper bound of stress accumulation is given by the failure stress. Without water load excess stresses were suggested to be released by slow deformations. With the additional water load the underlying rock is stabilized because the least principal stress (vertical) is increased more than the greatest principal stress (horizontal). Now additional horizontal stresses can be stored by the rock, moving the stresses again towards the failure threshold. During rapid lowering of the lake level the least principal stress is reduced much more than the greatest principal stress so that failure can occur. According to this model the foci of the seismic events should be located in regions which are stabilized by the water load and destabilized during periods of falling water level. In the following this essential assumption is checked by calculating the load induced stresses and comparing them with the initial stress field assumed by Blum et al. (1977). The effect of elastic anisotropy as well as anisotropy caused by the jointed body of rock is not considered in the calculations.

The initial stress field in the vicinity of the Schlegeis-Reservoir is not known. In their model Blum et al. (1977) proposed maximum compression in the direction SSE-NNW which agrees with the regional stress field in Central Europe and in the Alps as derived from fault plane solutions of earthquakes (Ahorner et al. 1972; Müller 1977). It is also confirmed by geological observations of postcrystalline deformation along shear planes dipping approximately to the North and to the South (Mignon 1972). Therefore this direction of the maximum compression was also chosen for the model calculations. The least principal stress was assumed to be directed vertically.

The water load of the reservoir was approximated by 29 rectangular elements with constant and linearly varying load distribution and by 8 point forces. The arrangement of the elements is depicted in Fig. 5. Additionally, the bathymetry of the lake is shown by contour-lines at intervals of 50 m. The maximum water level is reached at 1782 m above sea level.

Results of the calculations are shown along a vertical and a horizontal cross section (Figs. 6–7). The vertical plane crosses the reservoir about 0.2 km south of the dam (see Fig. 5). In the upper part of Fig. 6 the distribution of $\Delta\tau_0$ is shown for a water level of 1772 m which was reached in April 1974 at the beginning of the tremor series from which epicenter determi-

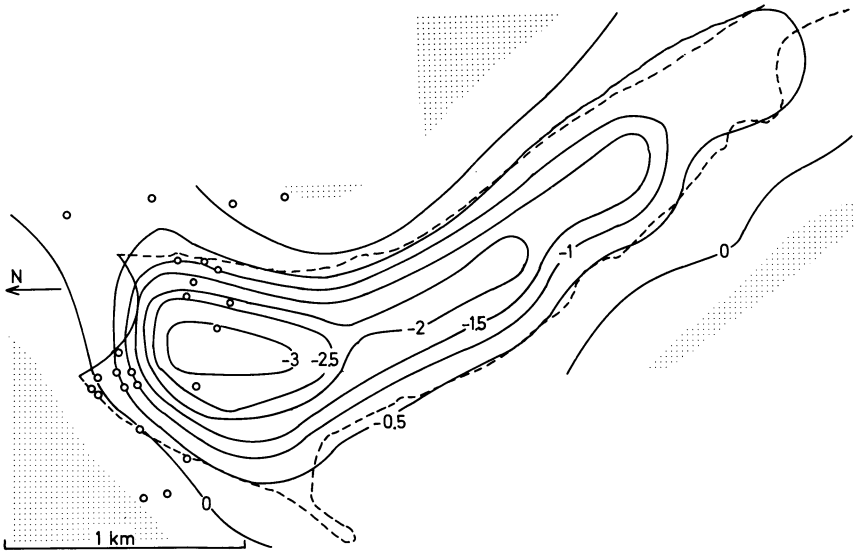

Fig. 7. Change of initial maximum shear stress, given in intervals of 0.5 bar, along a horizontal cross section at a depth of 1482 m. The lake level is at 1782 m. *Stippled:* regions destabilized by the filling of the reservoir. Circles denote epicenters of local tremors as located by Blum (1975)

nations are available. In the lower part of the figure the distribution of $\Delta\tau_0$ is shown for the maximum water level of 1782 m. Circles mark the epicenters of the tremors; they were projected on the cross section. Focal depths could not be determined as accurately as the epicenters. Therefore, upper and lower bounds of focal depths are given. With the initial stress direction assumed the rock within the reservoir region is stabilized by the water load ($\Delta\tau_0$ negative). The initial maximum shear stress τ_0 is diminished by more than 2 bar (Fig. 6), south of the profile even by more than 3 bar (see Fig. 7). The transition to the zones destabilized by the water load begins near the shore and extends landward to greater depths. At the maximum lake level τ_0 is increased by more than 0.5 bar. The tremor foci are situated in the transition zone between the stabilized and the destabilized region. During periods of falling water level the zones within the reservoir region are destabilized with respect to the period of maximum water level. If the model of Blum et al. (1977) were correct, an accumulation of hypocenters would be expected in these zones and not where they are actually located. Similar results have been found for two different initial stress fields: (1) for a stress field leading to EW strike slip motions along the nearly vertically dipping schist plane at Schlegeis and (2) for the stress field due to the weight of the surrounding mountains (Bock 1978). Therefore the model of dynamic stress equilibrium is not confirmed by the stress calculations carried out.

The increase of pore pressure at depth produced by the rise of the lake level is also not suited to explain the Schlegeis tremors for the following reason. This model would require rock permeabilities of the order of 0.01 millidarcy to explain the time lag of 4–6 months between the maximum water level and the occurrence of seismic events (Bock 1978). Such a low permeability is unlikely. Permeabilities for compact granite are of the order of 1 millidarcy and are increased by several orders of magnitude if the rock is fractured (Louis 1967). Seepage flow measurements in the vicinity of the Schlegeis dam also indicate higher permeabilities of the basement rock (Widmann and Heigerth 1976).

The characteristic features of the seismic activity observed at Schlegeis can be explained better by a model which was suggested after seismic events quite similar to those at Schlegeis have been also observed at other reservoirs in the Alps and in the Rumanian Carpathians (Merkler et al. 1978; Bock 1978). In the following this model is briefly described. A broader discussion will be given in a forthcoming paper (Merkler et al. in preparation). Cracks very close to the surface are water-filled by the reservoir. In the period of falling water level – i.e., in winter and springtime – the thermal insulation provided by the lake is removed and the water in the cracks can freeze at lower temperatures. This process leads to an increase in water volume. The stresses near the end of the cracks can be high enough to exceed the rock strength. This model does not only explain the temporal but also the spatial distribution of epicenters situated clearly outside the region of the actual shoreline (see Fig. 6 top).

Conclusions

The significance of the primary stress field for load induced seismicity has been demonstrated for a lake model of simple geometry. If the primary stress directions are known regions can be marked where the stresses are moved closer to the failure threshold. Taking into account the finite dimensions of a reservoir, earthquakes can in principle also be triggered in a tectonic environment of transcurrent and thrust faulting by the water load alone. Under the assumption of an initial stress direction favouring thrust faulting a model was checked which was proposed by Blum et al. (1977) to explain the mechanism of seismic events observed at the Schlegeis-Reservoir, Austria. It could be shown that the tremor foci are situated predominantly outside the regions which are stabilized by the increasing water load, where the foci should be located according to the model. Therefore, this model has been rejected as a viable hypothesis to explain the Schlegeis tremors.

Acknowledgements. These studies have been supported by the Deutsche Forschungsgemeinschaft (German Research Society) within the rock mechanics research program SFB 77 at Karlsruhe University. Computing facilities were made available by the computer center of Karlsruhe University. The author is indebted to Professor K. Fuchs, Dipl. Geol. G. Merkler, and Dr. G. Müller for many helpful discussions, and Professor K. Fuchs, Professor C. Kisslinger, and Dr. G. Müller for reading the manuscript.

Appendix

The stresses due to a distributed normal loading $p(x, y)$ on the surface $z=0$ of the semi-infinite solid $z>0$ are obtained by integration of the Boussinesq equations over a region F at the surface. In cartesian coordinates this leads to (Jaeger and Cook 1971, p. 282):

$$\sigma_x=\frac{1}{2\pi}\iint_F\left\{\frac{3(x-\xi)^2 z}{\rho^5}+(1-2\nu)\left[\frac{(y-\eta)^2+z^2}{\rho^3(z+\rho)}-\frac{z}{\rho^3}-\frac{(x-\xi)^2}{\rho^2(z+\rho)^2}\right]\right\}\cdot p(\xi,\eta)\,d\xi\,d\eta$$

$$\sigma_y=\frac{1}{2\pi}\iint_F\left\{\frac{3(y-\eta)^2 z}{\rho^5}+(1-2\nu)\cdot\left[\frac{(x-\xi)^2+z^2}{\rho^3(z+\rho)}-\frac{z}{\rho^3}-\frac{(y-\eta)^2}{\rho^2(z+\rho)^2}\right]\right\}\cdot p(\xi,\eta)\,d\xi\,d\eta$$

$$\sigma_z=\frac{3z^3}{2\pi}\iint_F\frac{p(\xi,\eta)}{\rho^5}\,d\xi\,d\eta$$

$$\tau_{yz}=\frac{3z^2}{2\pi}\iint_F\frac{(y-\eta)}{\rho^5}p(\xi,\eta)\,d\xi\,d\eta$$

$$\tau_{xz}=\frac{3z^2}{2\pi}\iint_F\frac{(x-\xi)}{\rho^5}p(\xi,\eta)\,d\xi\,d\eta$$

$$\tau_{xy}=\frac{1}{2\pi}\iint_F\left\{\frac{3z(x-\xi)\,(y-\eta)}{\rho^5}-(1-2\nu)\cdot\frac{(x-\xi)(y-\eta)(z+2\rho)}{\rho^3(z+\rho)^2}\right\}\cdot p(\xi,\eta)\,d\xi\,d\eta.$$

The normal force $p(\xi,\eta)\,d\xi\,d\eta$ acts at the point $(\xi,\eta,0)$. The distance to a field point (x, y, z) in the halfspace is given by $\rho=[(x-\xi)^2+(y-\eta)^2+z^2]^{1/2}$. For a constant vertical load $p(\xi,\eta)=p_0$ over a rectangular area $(0\leqq\xi\leqq l, 0\leqq\eta\leqq b)$ the following expressions for the stresses at the point $(0, 0, z)$ are obtained:

$$\sigma_z=\frac{p_0}{2\pi}\left[\arctan\frac{lb}{zR_3}+\frac{lbz}{R_3}\left(\frac{1}{R_1^2}+\frac{1}{R_2^2}\right)\right]$$

$$\sigma_x=\frac{p_0}{2\pi}\left[\arctan\frac{bl}{zR_3}-\frac{blz}{R_1^2R_3}-(1-2\nu)K_x\right]$$

$$\sigma_y=\frac{p_0}{2\pi}\left[\arctan\frac{lb}{zR_3}-\frac{lbz}{R_2^2R_3}-(1-2\nu)L_y\right]$$

$$\tau_{yz}=\frac{p_0}{2\pi}\left[\frac{l}{R_1}-\frac{z^2l}{R_2^2R_3}\right]$$

$$\tau_{xz}=\frac{p_0}{2\pi}\left[\frac{b}{R_2}-\frac{z^2b}{R_1^2R_3}\right]$$

$$\tau_{xy}=\frac{p_0}{2\pi}\left[1+\frac{z}{R_3}-z\left(\frac{1}{R_2}+\frac{1}{R_1}\right)-(1-2\nu)\ln\frac{(z+R_1)(z+R_2)}{2z(z+R_3)}\right]$$

with

$$R_1=\sqrt{l^2+z^2}$$
$$R_2=\sqrt{b^2+z^2}$$
$$R_3=\sqrt{l^2+b^2+z^2}$$
$$K_x=\arctan\frac{zb}{lR_3}+\arctan\frac{bl}{zR_3}-\arctan\frac{b}{l}$$
$$L_y=\arctan\frac{zl}{bR_3}+\arctan\frac{lb}{zR_3}-\arctan\frac{l}{b}.$$

For points other than $(0, 0, z)$ stresses are obtained by employing the principle of superposition (Poulos and Davis 1974, p. 12).

For a linearly varying vertical load over a rectangular area it is assumed that the load increases from zero at $(0, 0\leqq y\leqq b)$ to p_0 at $(l, 0\leqq y\leqq b)$. This leads to $p(\xi,\eta)=p_0(\xi/l)$. The stresses at (x, y, z) are given by

$$\sigma_x=\frac{p_0}{2\pi l}\left\{\frac{(x-l)zl}{r_1^2}\left(\frac{y}{R_1}-\frac{y-b}{R_3}\right)+xA+2zB+(1-2\nu)\left[lA_3-xA-zB+(y-b)C-yD+\frac{x-l}{2}\ln\frac{(x-l)^2+(y-b)^2}{(x-l)^2+y^2}-\frac{x}{2}\ln\frac{x^2+(y-b)^2}{x^2+y^2}+\frac{y}{2}E-\frac{y-b}{2}F+\frac{z}{2}G\right]\right\}$$

$$\sigma_y=\frac{p_0}{2\pi l}\left\{xA+\frac{(y-b)z}{r_2^2}\left(R_2-\frac{R_2^2}{R_3}+\frac{xl}{R_3}\right)-\frac{yz}{r_4^2}\left(R_0-\frac{R_0^2}{R_1}+\frac{xl}{R_1}\right)+zB-(1-2\nu)\left[x(A+A_1-A_2-C+D)-\frac{y-b}{2}F_1-(y-b)F_2+yE_2+\frac{y}{2}E_1+\frac{z}{2}G\right]\right\}$$

$$\sigma_z=\frac{p_0}{2\pi l}\left\{xA+\frac{x(x-l)(y-b)z}{R_3}\left(\frac{1}{r_2^2}+\frac{1}{r_1^2}\right)-\frac{x(x-l)yz}{R_1}\left(\frac{1}{r_4^2}+\frac{1}{r_1^2}\right)-\frac{x^2(y-b)z}{R_2}\left(\frac{1}{r_2^2}+\frac{1}{r_3^2}\right)+\frac{x^2yz}{R_0}\left(\frac{1}{r_4^2}+\frac{1}{r_3^2}\right)+\frac{z^3}{r_1^2}\left(\frac{y-b}{R_3}-\frac{y}{R_1}\right)-\frac{z^3}{r_3^2}\left(\frac{y-b}{R_2}-\frac{y}{R_0}\right)\right\}$$

$$\tau_{yz}=\frac{p_0}{2\pi l}\left\{\frac{xz^2}{r_4^2}\left(\frac{x-l}{R_1}-\frac{x}{R_0}\right)+\frac{xz^2}{r_2^2}\left(\frac{x}{R_2}-\frac{x-l}{R_3}\right)+z^2\left(\frac{1}{R_1}-\frac{1}{R_0}-\frac{1}{R_3}+\frac{1}{R_2}\right)\right\}$$

$$\tau_{xz}=\frac{p_0}{2\pi l}\left\{\frac{z^2l}{r_1^2}\left(\frac{y}{R_1}-\frac{y-b}{R_3}\right)-zA\right\}$$

$$\tau_{xy}=\frac{p_0}{2\pi l}\left\{zl\left(\frac{1}{R_3}-\frac{1}{R_1}\right)+zH-(1-2\nu)\left[\frac{x}{2}(F_1-E_1)+x(F_2-E_2)-y(A_2-D)+(y-b)(A_1-C)-zH\right]\right\}$$

with

$$R_0^2=x^2+y^2+z^2$$
$$R_1^2=(x-l)^2+y^2+z^2$$
$$R_2^2=x^2+(y-b)^2+z^2$$
$$R_3^2=(x-l)^2+(y-b)^2+z^2$$
$$r_0^2=x^2+y^2$$
$$r_1^2=(x-l)^2+z^2$$
$$r_2^2=(y-b)^2+z^2$$
$$r_3^2=x^2+z^2$$
$$r_4^2=y^2+z^2$$

$$A = \arctan\frac{(x-l)(y-b)}{zR_3} - \arctan\frac{(x-l)y}{zR_1} - \arctan\frac{x(y-b)}{zR_2} + \arctan\frac{xy}{zR_0}$$

$$A_1 = \arctan\frac{z(x-l)}{(y-b)R_3} - \arctan\frac{zx}{(y-b)R_2}$$

$$A_2 = \arctan\frac{z(x-l)}{yR_1} - \arctan\frac{zx}{yR_0}$$

$$A_3 = \arctan\frac{y-b}{x-l} - \arctan\frac{y}{x-l} - \arctan\frac{z(y-b)}{(x-l)R_3} + \arctan\frac{zy}{(x-l)R_1}$$

$$B = \ln\frac{y-b+R_3}{y-b+R_2} + \ln\frac{y+R_0}{y+R_1}$$

$$C = \arctan\frac{x-l}{y-b} - \arctan\frac{x}{y-b}$$

$$D = \arctan\frac{x-l}{y} - \arctan\frac{x}{y}$$

$$E = E_1 + E_2$$

$$E_1 = \ln\frac{(r_4^2 - zR_1)^2 + y^2(x-l)^2}{(r_4^2 - zR_0)^2 + y^2x^2} \qquad E_2 = \ln\frac{x^2+y^2}{(x-l)^2+y^2}$$

$$F_1 = \ln\frac{(r_2^2 - zR_3)^2 + (y-b)^2(x-l)^2}{(r_2^2 - zR_2)^2 + (y-b)^2x^2} \qquad F_2 = \ln\frac{x^2+(y-b)^2}{(x-l)^2+(y-b)^2}$$

$$G = \ln\frac{(r_4^2 - yR_1)^2 + z^2(x-l)^2}{(r_4^2 - yR_0)^2 + z^2x^2} - \ln\frac{(r_2^2 - [y-b]R_3)^2 + z^2(x-l)^2}{(r_2^2 - [y-b]R_2)^2 + z^2x^2}$$

$$H = \ln\frac{x-l+R_3}{x-l+R_1} + \ln\frac{x+R_0}{x+R_2}.$$

References

Ahorner, L., Murawski, H., Schneider, G.: Seismotektonische Traverse von der Nordsee bis zum Apennin. Geol. Rundsch. **61**, 915–942, 1972

Bell, M.L., Nur, A.: Strength changes due to reservoir-induced pore pressure and stresses and application to Lake Oroville. J. Geophys. Res. **83**(B9), 4469–4483, 1978

Blum, R.: Seismische Überwachung der Schlegeis-Talsperre und die Ursache induzierter Seismizität. Diss., Universität Karlsruhe, 1975

Blum, R., Bock, G., Fuchs, K., Merkler, G., Widmann, R.: Correlation between micro-activity and variation of water level at the Schlegeis-Reservoir. J. Geophys. **43**, 561–567, 1977

Blum, R., Fuchs, K.: Observation of low-magnitude seismicity at a reservoir in the Eastern Alps. Eng. Geol. 8, 99–106, 1974

Bock, G.: Induzierte Seismizität: Modelle und die Beobachtungen am Schlegeis- und Emosson-Stausee. Diss., Universität Karlsruhe, 1978

Bufe, C.G.: The Anderson Reservoir seismic gap – induced aseismicity? Eng. Geol. **10**, 255–262, 1976

Comninakis, P., Drakopoulos, J., Moumoulidis, G., Papazachos, B.: Foreshock and aftershock sequences of the Kremasta earthquake and their relation to the water-loading of the Kremasta artificial lake. Ann. Geofis. **21**, 39–71, 1968

Gough, D.I.: Incremental stress under a two-dimensional artificial lake. Can. J. Earth Sci. **6**, 1067–1075, 1969

Gough, D.I., Gough, W.I.: Stress and deflection in the Lithosphere near Lake Kariba – I. Geophys. J.R. Astron Soc. **21**, 65–78, 1970a

Gough, D.I., Gough, W.I.: Load-induced earthquakes at Lake Kariba – II. Geophys. J. R. Astron. Soc. **21**, 79–101, 1970b

Gupta, H.K., Narain, H., Rastogi, B.K., Mohan, I.: A study of the Koyna earthquake of December 10, 1967. Bull. Seismol. Soc. Am. **59**, 1149–1168, 1969

Gupta, H.K., Rastogi, B.K.: Dams and earthquakes. Amsterdam: Elsevier 1976

Handin, J.: Strength and ductility. In: Handbook of physical constants, S.P. Clark Jr., ed.: pp. 223–289. Geol. Soc. Am. Mem. **97**, 1966

Hubbert, M.K., Rubey, W.W.: Mechanic of fluid-filled porous solids and its application to overthrust faulting. Bull. Geol. Soc. Am. **70**, 115–166, 1959

Jaeger, J.C., Cook, N.G.W.: Fundamentals of rock mechanics. London: Chapman and Hall Ltd., Science Paperback 1971

Kisslinger, C.: A review of theories of mechanisms of induced seismicity. Eng. Geol. **10**, 85–98, 1976

Lee, T.: A method for computing the deformation of the crust caused by the filling of large lakes. Bull. Seismol. Soc. Am. **62**, 1597–1610, 1972

Louis, C.: Strömungsvorgänge in klüftigen Medien und ihre Wirkung auf die Standsicherheit von Bauwerken und Böschungen im Fels. Veröffentlichungen Inst. f. Bodenmechanik und Felsmechanik der Universität Karlsruhe **30**, 1967

Merkler, G., Bock, G., Fuchs, K.: Ice-induced seismic microactivity at reservoirs (Abstract). ESC-Meeting, Strasbourg, September 1978

Mignon, K.: Überblick über die geologischen Verhältnisse. Österr. Z. Elektrizitätswirtschaft **25**, 432–436, 1972

Müller, G.: Fault-plane solution of the earthquake in Northern Italy, 6 May 1976, ans implications for the tectonics of the Eastern Alps. J. Geophys. **42**, 343–349, 1977

Poulos, H.G., Davis, E.H.: Elastic solutions for soil and rock mechanics. New York: J. Wiley & Sons 1974

Nyland, E., Withers, R.J.: A fast method for computing load induced stress in the Earth. Geophys. J.R. Astron. Soc. **44**, 689–698, 1976

Raleigh, C.B., Healy, J.H., Bredehoeft, J.D.: An experiment in earthquake control at Rangely, Colorado. Science **191**, 1230–1237, 1976

Simpson, D.W.: Seismicity changes associated with reservoir loading. Eng. Geol. **10**, 123–150, 1976

Snow, D.T.: Geodynamics of seismic reservoirs. Proc. Symp. on percolation through fissured rocks, Int. Soc. Rock Mechanics, Stuttgart, T2-J, 1–19, 1972

Widmann, R., Heigerth, G.: Rock deformation and seepage flow in the foundation of the Schlegeis arch dam. Comm. Inter. des Grands Barranges, 12ième Congrès, Mexico, Q.45, R.39, 1976

Widmann, R., Schlosser, J., Stäuble, H.: Die Bogengewichtsmauer Schlegeis. Österr. Z. Elektrizitätswirtschaft **25**, 395–404, 1972

Withers, R.J., Nyland, E.: Theory for the rapid solution of ground subsidence near reservoirs on layered and porous media. Eng. Geol. **10**, 169–185, 1976

Received July 25, 1979; Revised Version December 20, 1979